MM Science Journal | www.mmscience.eu
ISSN 1803-1269 (Print) | ISSN 1805-0476 (On-line)
Special Issue | HSM 2019
15th International Conference on High Speed Machining
October 8-9, 2019, Prague, Czech Republic
DOI: 10.17973/MMSJ.2019_11_2019093

HSM2019-128

MODELLING AND OPTIMIZATION OF THE CUTTING FORCES DURING TI6AL4V MILLING PROCESS USING THE RESPONSE SURFACE METHODOLOGY AND DYNAMOMETER

I. A. Daniyan[1]*, I. Tlhabadira[2], S. N. Phokobye[3], M. Siviwe[3], K. Mpofu[1]

[1]Department of Industrial Engineering, Tshwane University of Technology, Pretoria, South Africa

[2]Department of Mechanical & Mechatronics Engineering, Tshwane University of Technology, Pretoria, South Africa

[3]Institute of Advanced Tooling, Tshwane University of Technology, Soshanguve, South Africa

*Corresponding author; e-mail: afolabiilesanmi@yahoo.com

Abstract
The measurement of cutting forces using highly sensitive piezoelectric force sensors is significant in the optimization of the machining process. In this study, the modelling and optimization of the cutting forces during the milling process of Ti6Al4V was carried out using the Response Surface Methodology (RSM) and the dynamometer. The ranges of the process parameters are: cutting speed (250-280 mm/min), feed per tooth (0.06-0.24 mm) and axial depth of cut (0.30-3.0 mm) are varied over four levels while cutting force serves as the response of the designed experiment. The physical experiments were carried out using a DMU80monoBLOCK Deckel Maho 5-axis CNC milling. Three sets of 2- flute, 10 mm corner radius mills was used for the machining operation. A solid rectangular work piece of Ti6Al4V was screwed to the stationary dynamometer (KISTLER 9257A 8-Channel Summation of Type 5001A Multichannel Amplifier) mounted directly to the machine table. Milling operations were performed using different cutting parameters of cutting speed, feed per tooth and depth of cut and data were collected through Data Acquisition (DAQ) connected to the computer. The numerical experiment produced a mathematical model for predicting the values of the cutting forces as a function of the independent process parameters while the physical experiment revealed that the piezoelectric sensor is highly sensitive to variations in the values of the cutting force.

Keywords:
Cutting speed; Depth of cut; Feed; Piezoelectric sensors; Process parameters

1 INTRODUCTION

The mechanics of cutting considers the machining process and accurate estimation of the machining forces using the appropriate models. The cutting force is the force required to shear the work piece, which is impacted by the cutting tool during machining operation. The determination of the appropriate cutting force is important in the selection of face or end mill cutter as cutting force differs with the tool geometry and orientation [Altintas 2012; Grossi et al., 2015; Rubeo and Schmitz, 2016]. The tool's geometry influences the force required for machining work piece and chip separation. Cutting forces generally falls into three categories; the normal force, which acts radially or axially [Aquici et al., 2012; Mehdi and Zghal, 2011; Wen et al., 2013]. This force pushes the tool away from the work piece in the axial or radial direction and accounts for approximately 10% of the total cutting forces during the machining process. The axial force components acts in the direction parallel to the machine's spindle while the radial force components acts in the direction perpendicular to the spindle of the milling machine. Milling machines are often designed for rigidity in order to withstand the axial force components and indexable cutting tools are designed to generate more axial forces than the radial forces hence the radial forces are what causes chatter by pushing the tool off the work piece centre in most cases. On the other hand, the feed forces acts directly on the tool in the direction that is parallel to the direction of the feed and accounts for about 20% of the total cutting forces during. In addition, the tangential forces acts on the rake face of the milling cutter in the direction of the cutting velocity and accounts for a significant amount of the total forces generated during the milling operation. The tangential forces decreases with the selection of a cutter with large positive axial rake decreases and vice versa [Yang et al., 2011; Rychokov and Yanyushkin, 2016; Burek et al., 2017]. However, the

magnitude of the cutting force components depends on the cutting edge geometry and engagement conditions. Titanium alloys are characterized with excellent mechanical properties such as good hardness, ductility, and corrosion resistance but they are generally referred to as “difficult to machine materials” because of its low thermal conductivity which often requires high cutting force and may result in tool wear and poor surface finish [López de Lacalle et al., 2006; González et al. 2018]. There is need for cutting force measurement, prediction and control in order to enhance product quality, optimum cutting tool performance and cost effectiveness of the tool and the cutting process. This is because the cutting force can significantly affect the surface finish requirements of the work piece creating chatter and burr, and can increase the energy requirements of the cutting operation as well as affect the useful life of the cutting tool, hence, the need for control [Scippa et al., 2015; Mejri and Mehdi, 2018; Wan et al., 2016]. The cutting force represent a critical design metric because it determines the required spindle power, torque and the rigidity of the machine tool’s structural loop. The modelling of the cutting forces involves the mathematical representation of the machining process in order to determine the influence of varying process parameters on the cutting forces by approximate or exact solutions. Many researchers have reported on the modelling and optimization of cutting forces and other process parameters during the machining operations, using different approaches. For instance, the use of analytical approach [López de Lacalle et al., 2006; Urbikan et al. 2017; González et al. 2018] and numerical models such as the Response Surface Methodology, Taguchi and Generic Algorithm [Dikshit et al., 2014; Ribeiro et al., 2017], Artificial Neural Network [Karabulut, 2015], Fuzzy rules based models [Nandi 2012], analytical models [Jing et al., 2014; Perez et al., 2013; Altintas and Lee, 1996], adaptive linear control systems [Leal-Muñoza et al., 2018; Orra and Choudhury, 2015], have been reported. [Urbikan et al. 2017] carried out the numerical simulation of milling forces with barrel-shaped tools considering runout and tool inclination angles. The mathematical model was used to describe and predict the behaviour for barrel-shaped tools. This model was based on the numerical dis- cretization of the edge elements, which includes the basic geometrical parameters, lead and tilt rotation angles as well as variable runout consideration. Furthermore, many authors have also proposed the use of sensors for the optimization of processes related to cutting conditions, in order to determine the state of the machine and to monitor tool wear, among others. This will enhance quick decisions making in real time in order to improve the efficiency of the process [Giorgio et al., 2016; Ratnam et al., 2016]. During the machining process simulation and optimization, cutting force modelling strongly determines the accuracy of the results obtained [Zhu et al., 2014; Zhu and Mao, 2015]. The determination of the appropriate cutting force for any milling operation depends on the type of milling process (face or end milling, shoulder milling, feed or slot milling operations) as well as the mechanical and thermal properties of the work piece and the geometry of the cutting tool employed (the rake and helix angles as well as the nature of coatings). However, the development and use of the appropriate cutting force models can assist in the selection of the right process parameters such as the speed rate and spindle speed during the machining operations [Wojciechowski et al., 2016; Ghorbani and Moetakef-Imani, 2016]. This work considers the use of both the physical and numerical experimentations in measuring and predicting the cutting force during machining operations. The cutting process is a very dynamic process with fluctuations and interruptions, which can affect the surface finish and the dimensional tolerance of the product hence the use of high natural frequency piezoelectric sensors, permits the detection in the variation of cutting forces for both low and high speed machining operations. The measurement of cutting force is important in that it helps in the optimization of tool life, machinability of work piece, determination of the right tool geometry and coatings, prevention of wear and vibration and investigation of the nature of chips produced which is highly essential in meeting the surface finish requirements. The dynamometer used in this work is an emerging product that is highly resistive to thermal and signal drift in contrast with previous generations of dynamometers, which is prone to thermal and signal drift used by previous researchers. In addition to this, the mathematical model developed for correlating and predicting the cutting force as a function of the independent process parameters during the milling operation of Ti6Al4V has not been sufficiently reported by the existing literature.

2 MATERIALS AND METHOD

2.1 The design of the numerical experiment

The design of the numerical experiment was carried out using the Response Surface Methodology (RSM) and the Central Composite Design (CCD) in order to determine the feasible combinations of process parameters and the significance of each as well as effects of their interactions on the cutting force. The RSM is a mathematical and statistical technique usually employed for numerical modelling of numerical experiments in order to determine the optimum process condition and the influence of process parameters on the output response and to determine the optimum condition [Bello et al., 2016]. The ranges of the process parameters are cutting speed (250-280 mm/min), feed per tooth (0.06-0.24 mm) and axial depth of cut (0.30-3.0 mm) are varied over four levels while cutting force serves as the response of the designed experiment. The statistical analysis of the results obtained produced a mathematical model, which correlates the cutting

force as a function of the independent process parameters. The choice of the low cutting speed stems from the fact that the cutting of titanium often causes vibration, deflection and chatter when subjected to high-speed cutting pressure and the spring-back induces cutting edge failure and vibration [Ezugwu and Wang, 1997]. Furthermore, the growth of flank wear grows linearly between 20 to 200 m/min of cutting speed for Ti6Al4V and for 250 m/min the flank wear growth found to have an exponential increase [Nurul, 2007]. This challenge can be overcome using specially designed cutting tool such as the Polycrystalline Diamond (PCD) and Polycrystalline Cubic Boron Nitride (PCBN) cutting tools. Hence, the choice of the low cutting speed is to enhance good surface finish and dimension accuracy.

2.2 The physical experiment

The physical experiments were carried out using a DMU80monoBLOCK Deckel Maho 5-axis CNC milling. Three sets of 2- flute, 10 mm corner radius mill cutter was used for the machining operation. A solid rectangular work piece of Ti6Al4V was screwed to the stationary dynamometer (KISTLER 9257A 8-Channel Summation of Type 5001A Multichannel Amplifier) mounted directly to the machine table. Milling operations were performed using different cutting parameters of cutting speed, feed per tooth and depth of cut and data were collected through Data Acquisition (DAQ) connected to the computer. The CNC milling used during the experiments has a maximum spindle speed of 18000 rpm, at a feed rate of 30000 mm/rev. The dynamometer uses piezoelectric sensors for measuring the cutting forces at high frequencies. Hence, it is highly sensitive allowing little fluctuations in the value of the cutting force to be easily detected. It also allows quick and visible detection of minor adjustment in the tool geometry, materials and coatings in a bid to optimize the overall machining process. Figure 1 illustrates the schematics of the experimental set up.

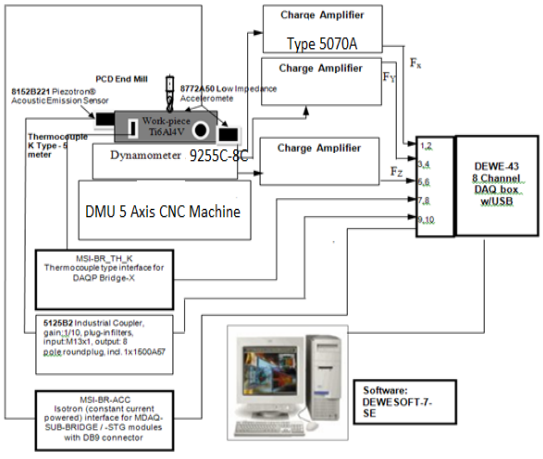

Fig. 1: The dynamometer set up for cutting force measurement.

The specifications of the cutting tool is presented in Table 1.

Tab. 1: The cutting tool specifications.

Symbol	Parameter	Value
T_d	Tool diameter (mm)	10
F_l	Flute length (mm)	15
F_n	Number of flute	2
L	Overall length(mm)	58
β	Helix angle (°)	30
n	Number of teeth	2
β_1	Axial rake angle	15°
β_2	Radial rake angle	15°
α	Cutting edge angle	10°
θ	Clearance angle	10°
φ	Relief angle	10°

The cutting force model is expressed as Equations 1-10 as proposed by Altinta and Lee [23] and Bhaohao et al [7].

$$dF_{j,T}(\phi_j,z) = f_{T,}b(\phi_j,z)db \quad (1)$$

$$dF_{j,R}(\phi_j,z) = f_{R,}b(\phi_j,z)db \quad (2)$$

$$dF_{j,A}(\phi_j,z) = f_{A,}b(\phi_j,z)db \quad (3)$$

Where $f_{T,}$ $f_{R,}$and f_A are the tangential, radial and axial cutting force coefficients, $b(\phi_j,z)$ is the chip thickness, dz is the differential length, db is the length of the cutting flute, ϕ_j is the angular position of the jth tooth at elevation z expressed as Equation 4.

$$\phi_j,z = \phi_j = \phi_i(z) + (j-1)\phi_p \quad (4)$$

$\phi_i(z)$ is the rotational angle of the reference flute measured from the Y axis, ϕ_p is the pitch angle expressed as Equation 5.

$$\phi_p = \frac{2\pi}{N} \quad (5)$$

Where N is the number of cutter teeth.

The orthogonal force components is expressed thus;

$$\begin{bmatrix} dF_{i,j,X}(\phi_j,z) \\ dF_{i,j,Y}(\phi_j,z) \\ dF_{i,j,Z}(\phi_j,z) \end{bmatrix} = K \begin{bmatrix} dF_{i,j,T} \\ dF_{i,j,R} \\ dF_{i,j,A} \end{bmatrix} \quad (6)$$

$$K = \begin{bmatrix} -\cos\phi_{ij} - sin\phi_{ij} & 0 \\ sin\phi_{ij} - \cos\phi_{ij} & 0 \\ 0 \quad 0 & -1 \end{bmatrix} \quad (7)$$

The total cutting force is expressed as Equation 8

$$F_j = \int_{y_1}^{y_2} dF_j dz \quad (8)$$

The total cutting force in all directions is expressed as Equation 9

$$F_{X,Y,Z} = \sum_{j=1}^{N} Fj \qquad (9)$$

The cutting forces F_x, F_y and F_z are measured directly using the dynamometer while the corresponding moments M_x, M_y and M_z are calculated from the individual force components and sensor distances a and b as expressed by Equations 10-15.

$$F_x = F_{x1+2} + F_{x3+4} \qquad (10)$$

$$F_y = F_{y1+4} + F_{y2+3} \qquad (11)$$

$$F_z = F_{z1} + F_{z2} + F_{z3} + F_{z4} \qquad (12)$$

$$M_x = b(F_{z1} + F_{z2} - F_{z3} - F_{z4}) \qquad (13)$$

$$M_y = a(-F_{z1} + F_{z2} + F_{z3} - F_{z4}) \qquad (14)$$

$$M_y = b(-F_{x1+2} + F_{x3+4}) + a\,(F_{y1+4} - F_{y2+3}) \qquad (15)$$

3 RESULTS AND DISCUSSION

The combination of various process parameters as well as the corresponding actual cutting force from the physical experiment and the predicted cutting force from the numerical experiment is presented in Table 2.

Tab. 2: Combination of process parameters and the corresponding actual and predicted cutting force.

Run	Cutting speed (mm/min)	Feed per tooth (mm)	Depth of cut (mm)	Actual cutting force (N)	Predicted cutting force (N)
1	267.50	0.24	1.75	32.11	31.987
2	270	0.04	1.50	32.02	31.768
3	267.50	0.14	1.40	31.99	32.046
4	265	0.20	0.50	31.93	32.333
5	275	0.20	3.00	31.81	31.989
6	260	0.14	1.65	31.67	31.001
7	267.50	0.06	2.00	31.56	32.466
8	260	0.08	1.65	31.34	33.099
9	265	0.12	1.00	31.18	32.000
10	270	0.16	1.75	30.92	30.620
11	275	0.08	0.50	30.73	31.064
12	254.89	0.06	0.30	30.49	30.897
13	260	0.20	0.60	30.28	30.248
14	265	0.22	2.40	29.97	29.766
15	270	0.14	2.50	29.70	29.670
16	275	0.16	2.80	29.50	29.300
17	265	0.18	2.60	29.28	29.540
18	260	0.14	1.60	29.01	29.000
19	267.50	0.16	1.55	28.72	29.121
20	280.11	0.10	2.50	28.50	28.100

Using the 2FI and the regression models, the statistical analysis of the results presented in Table 2 produced a mathematical model for the prediction of cutting force as a function of the independent process parameters namely the cutting speed (V_c), feed per tooth (f) and axial depth of cut (d) (Equation 16)

$$Total\ cutting\ force = +30.63 - 0.031V_c + 0.43f + 0.27d + 0.35V_cf + 0.19V_cd + 0.33fd \qquad (16)$$

The degree of agreement between the values of cutting forces obtained from the physical experimentation and the ones obtained from the predictive model is shown in Figure 2. From the nature of plot, judging from similar data points there is high degree of agreement between the results obtained from the physical and numerical experiments. This point to the fact that the model terms of the developed model is highly significant for predictive purpose.

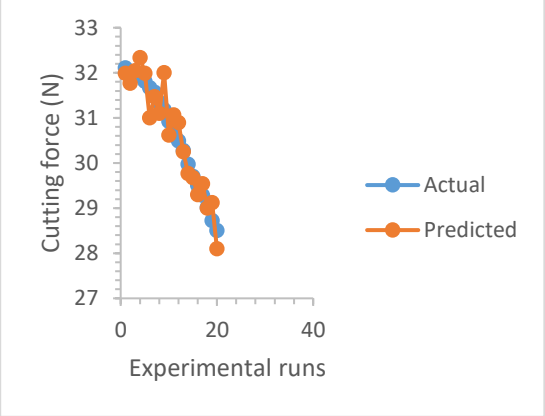

Fig. 2: Actual and predicted values of cutting force.

In addition, Tables 3 shows the results from the Analysis of Variance (ANOVA) for the predictive model. The model terms comprise of six factors terms namely; A, B C, AB, AC, BC, which are highly significant because of their influence on the values of the cutting force. At 95% confidence level of significance, the F-value was low (> 0.05). The F-values is an indication of the F distribution value used to compare the variances. It is the ratio of the model mean to the appropriate error mean square. When the value of F-value is less than 0.05, it implies that the effects of the process variables on the response (cutting force) are statistically significant. The coefficient of correlation (R^2) which measures of the magnitude of variation in the mean and the reduction of response variability gave (0.9857). This shows that 96.57 % of the total variance in the value of the cutting speed was influenced by the process parameters. The closer the value of the R^2 to 1, the more significant the model. Also, the adjusted R^2 which measures the overall variation in the data as indicated by the model gave 0.9700. This indicates that the model is highly significant without considering the introduction of additional terms. Furthermore, the standard deviation, which is a function of the variances within the model, was 6.7806×10^{-4}. The smaller value of standard deviation, the greater the significance of the model terms and vice versa. The difference between the

predicted R^2 (0.9857) and the adjusted R^2 (0.9700) is less than 0.2. For a good model, the values of its adjusted R-squared and the R-squared should be close to 1 and must be within the range of 0.2 to each other.

Tab. 3: Statistical parameters of the developed model.

Parameter	Value
Standard deviation	6.7806×10^{-4}
Mean	1.48
Coefficient of variation CV (%)	0.0465
Prediction error sum of square (PRESS)	2.134×10^{-5}
R-squared	0.9857
Adjusted R-squared	0.9700
Adequate precision	38.650

Figures 3 also shows the stochastic error and plot of residual errors as well as the actual values of the cutting speed and the corresponding predicted values. This is used to test the normality of the data to determine that the statistical analysis underlying the data analysis are significant. The presence of lack of fit up to 6 indicates that the developed model is adequate for correlation and predictive purpose.

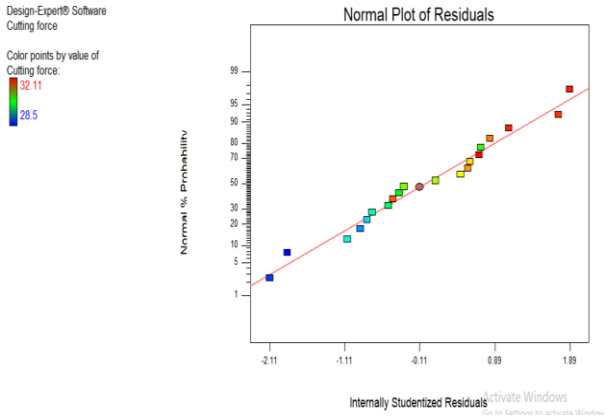

Fig. 3: The normal plot of residual errors.

Figures 4 and 5 show the 2D and 3D plots of the effect of feed per tooth and cutting speed on the cutting force. From the plots, it was observed that the cutting force increases with increase in feed per tooth and decreases with increase in the cutting speed and temperature. The feed per tooth is the distance the work piece is fed into the cutter as each tooth rotates. When the distance the work piece is fed into the cutter is small, the cutting force may reduce due to the fact that only some little portion of the work piece will experience the impact of the cutting force. The impact of the cutting force will be felt more when large portion of the work piece is fed for engagement with the cutting tool thereby increasing the cutting force. On the other hand, when the cutting speed increases, the temperature at the work piece-tool interface increases resulting in the reduction in the hardness of the work piece thereby reducing the cutting force required. Keeping the axial depth of cut constant at 1.75 mm, with the maximum and minimum values of the cutting force was found to be 31.1224 N and 30.0651 N respectively. From Figures 5 and 6, the optimum cutting force was found to be 30.6037 N. Below this value, the cutting force may be insufficient for the required cutting operation resulting in increase in the machining cycle time and poor surface finish. Above this value, the cutting force seems to be excessive as indicated by the portion of the plot in red colour. Excessive cutting force increases the energy consumption, promotes vibration, chatter, dimensional inaccuracy as well as reduction in the useful life of the tool.

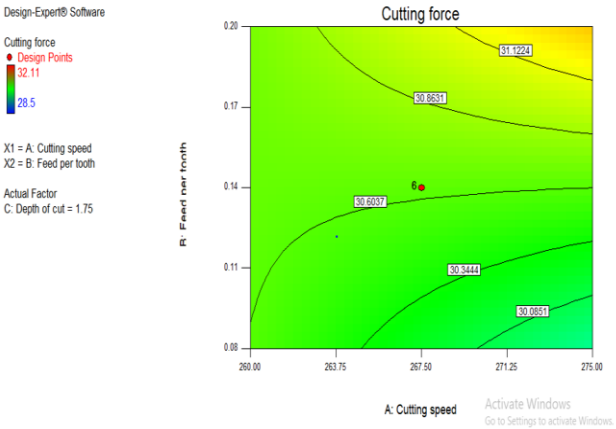

Fig. 4: The 2D plot of the cross effect of feed per tooth and cutting speed on the cutting force.

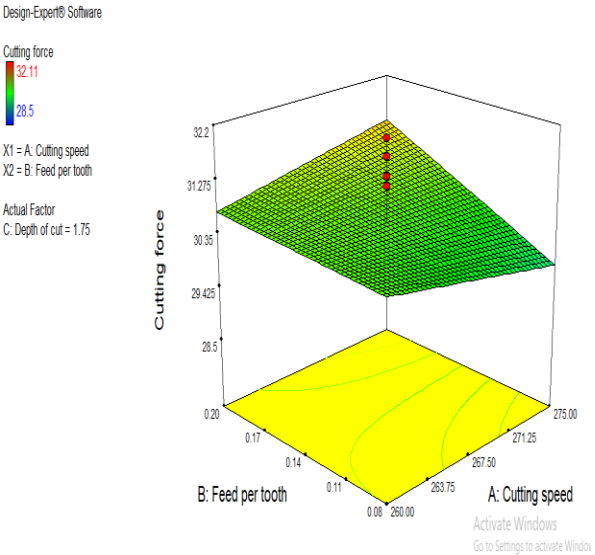

Fig. 5: The 3D plot of the cross effect of feed per tooth and cutting speed on the cutting force.

Figures 6 and 7 show the 2D and 3D plot of the cross effect of depth of cut and cutting speed on the cutting force respectively. An increase in the depth of cut increases the cutting force and vice versa while the cutting force reduces with increase in the cutting speed. The axial depth of cut measures the distance

penetrated by the cutter into the work piece along its centre line. As the axial depth of cut increases, the surface area to volume ratio decreases with decrease in frictional energy and resulting increase in the cutting force. Keeping the axial depth of cut constant at 0.14 mm, the maximum and minimum values of the cutting force was found to be 30.9073 N and 30.3002 N respectively. The optimum value of the cutting force was found to be 30.6037 N as values of cutting forces below or above this value may be insufficient or excessive for the required operation resulting in deformation of the tool and work piece with increase in the machining time.

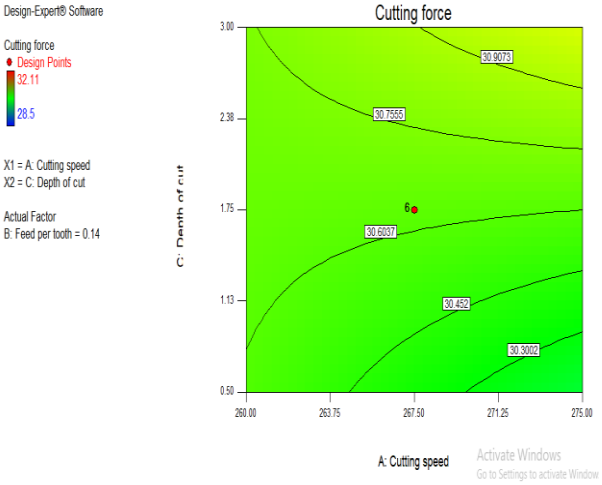

Fig. 6: The 2D plot of the cross effect of axial depth of cut and cutting speed on the cutting force.

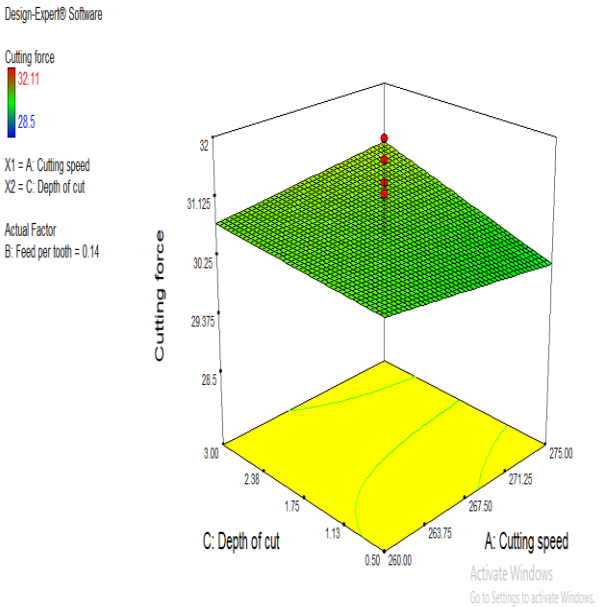

Fig. 7: The 3D plot of the cross effect of axial depth of cut and cutting speed on the cutting force.

Figures 8 and 9 show the 2D and 3D plot of the cross effect of axial depth of cut and feed per tooth on the cutting force respectively. An increase in the axial depth of cut and feed per tooth leads to an increase in the cutting force and vice versa. Keeping the cutting speed constant at 267.50 mm/min, the cutting force increases from 30.397 N to 31.4077 N as the axial depth of cut and feed per tooth increases. The optimum value of the cutting force was found to be 30.6497 N. The values of the cutting force below this value was found to be insufficient for the machining operation while values exceeding this threshold are no longer suitable for the required operation as indicated by the area marked with red colour in the plot. While insufficient cutting force may result in poor surface finish and increase in the machining cycle time, excessive cutting force may cause vibration, tool-work piece deflection and subsequently chatter leading to dimensional inaccuracy.

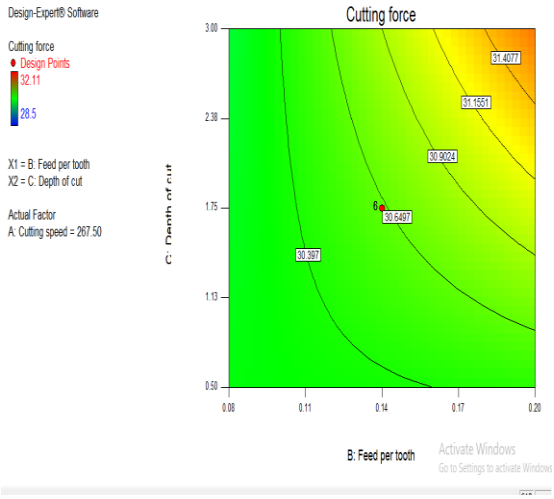

Fig. 8: The 2D plot of the cross effect of axial depth of cut and feed per tooth on the cutting force.

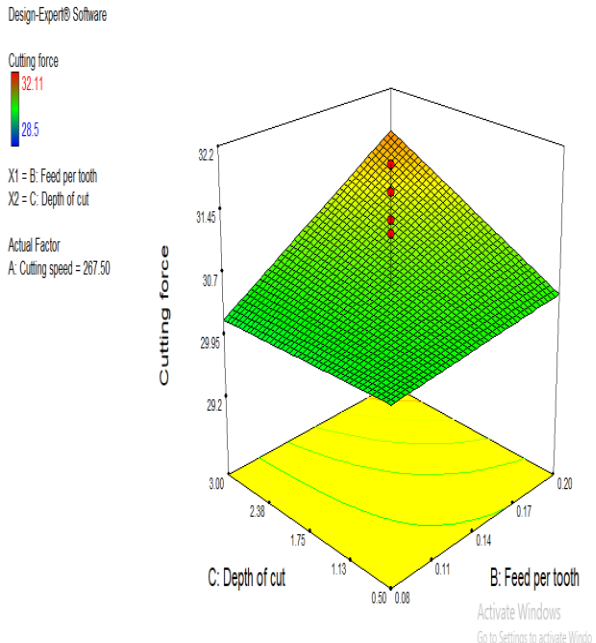

Fig. 9: The 3 plot of the cross effect of axial depth of cut and feed per tooth on the cutting force.

The three orthogonal shear force components in the x-direction (F_x) y-direction (F_y) and z-direction (F_z) were measured using the dynamometer while their corresponding moments M_x, M_y and M_z are calculated by the software (Table 4). The experiment was conducted with and without the use of coolant. The essence is to investigate the effect of coolants on the cutting force.

Tab. 4: Cutting forces and moments without the use of coolants.

Run	Time (S)	F_x (N)	F_y (N)	F_z (N)	M_x (Nm)	M_y (Nm)	M_z (N
1	0.000	-1.59	32.11	28.78	1.20	0.71	-0.
2	0.001	-1.60	32.02	28.62	1.39	0.63	-0.
3	0.002	-1.66	31.99	28.10	1.42	0.49	-0.
4	0.003	-1.64	31.93	27.72	1.27	0.63	-0.
5	0.004	-1.60	31.81	27.76	1.32	0.68	-0.57
6	0.005	-1.56	31.67	27.76	1.29	0.66	-0.56
7	0.006	-1.54	31.56	27.73	1.22	0.95	-0.74
8	0.007	-1.49	31.34	27.90	1.22	0.61	-0.57
9	0.008	-1.53	31.18	27.72	1.22	0.68	-0.50
10	0.009	-1.50	30.92	27.54	1.44	0.59	-0.55
11	0.010	-1.46	30.73	27.62	1.42	0.54	-0.46
12	0.011	-1.42	30.49	27.75	1.20	0.61	-0.57
13	0.012	-1.36	30.26	27.86	1.12	0.54	-0.49
14	0.013	-1.26	29.97	27.90	1.05	0.51	-0.56
15	0.014	-1.18	29.70	27.93	0.90	0.63	-0.57
16	0.015	-1.12	29.50	27.86	1.12	0.46	-0.60
17	0.016	-1.08	29.28	27.85	1.07	0.61	-0.
18	0.017	-1.01	29.01	28.16	0.85	0.63	-0.
19	0.018	-0.97	29.72	28.32	1.03	0.78	-0.
20	0.019	-0.96	28.50	28.30	1.00	0.66	-0.

Figure 10 shows the three orthogonal cutting force components F_x, F_y, F_z in the x, y and z directions respectively. The cutting force was highest along the vertical axis and least along the horizontal axis. The changes in the value of the cutting force is as a result of the periodic entry and exit of the cutting edge of the tool accompanied by varying chip thickness. The milling tool follows a rotary path and the simultaneous feed and rotating motion of the tool often leads to variation in the cutting force and chip thickness. In addition, the shape of the plot implies that the piezoeletric sensors used by the dynamometer is highly sensitive to little variations in the magnitude of the cutting forces.

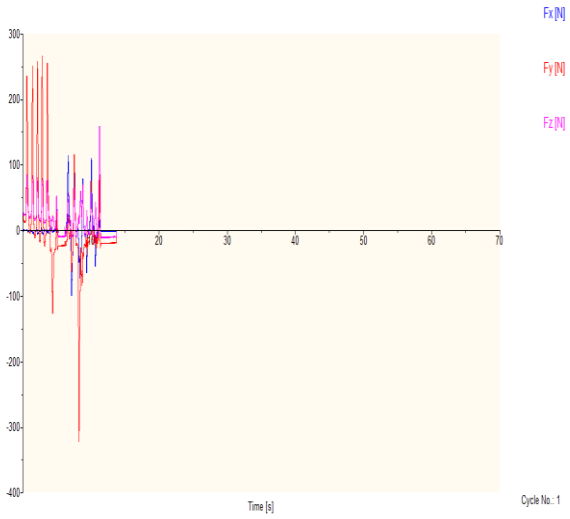

Fig. 10: The three orthogonal cutting force components without the use of coolants.

Figure 11 presents the three orthogonal cutting force components as well as the frequencies of the piezometric sensor. From the plot, it is clear that that due to the high natural frequency of the piezometric sensor, the measuring system is high sensitive to variations and fluctuations in the value of the cutting speed that is not up to unity.

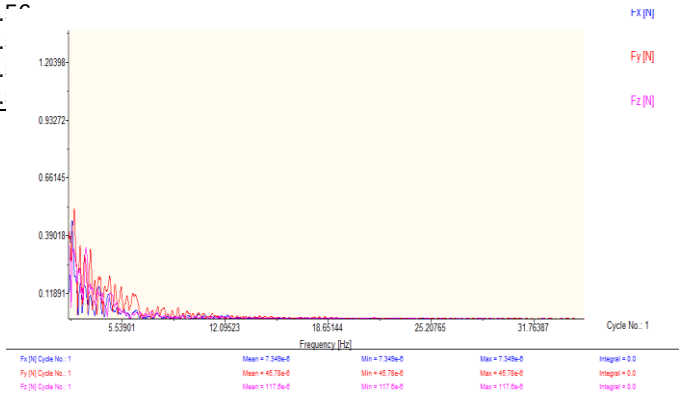

Fig. 11: Plot of the three orthogonal cutting forces and the frequency of the sensor with the use of coolants.

Figure 12 shows the moment of forces in the three orthogonal axes. The moment of forces, which is the product of the force and the perpendicular distance of the piezometric sensors (800 mm) reflects the magnitude of torque generated which is a function of the power and energy requirements of the machining process. The moment of forces as well as the torque generated was highest along the horizontal x-axis and least along the z-axis.

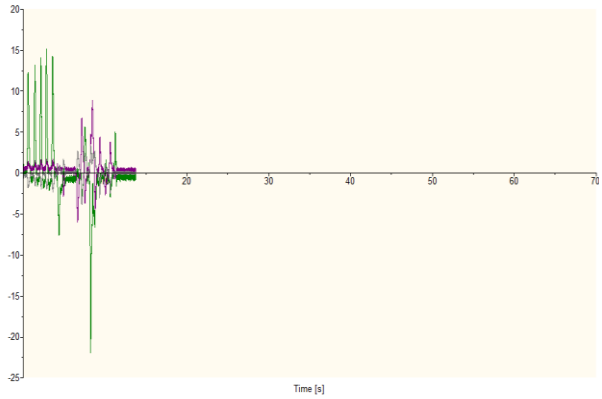

Fig. 12: The moment of forces in the three orthogonal axes with the use of coolants.

Figure 13 presents the plot of the moments of the cutting forces and the frequencies of the sensor. At high frequencies, the measuring system was sensitive enough to compute small values of the moment of forces.

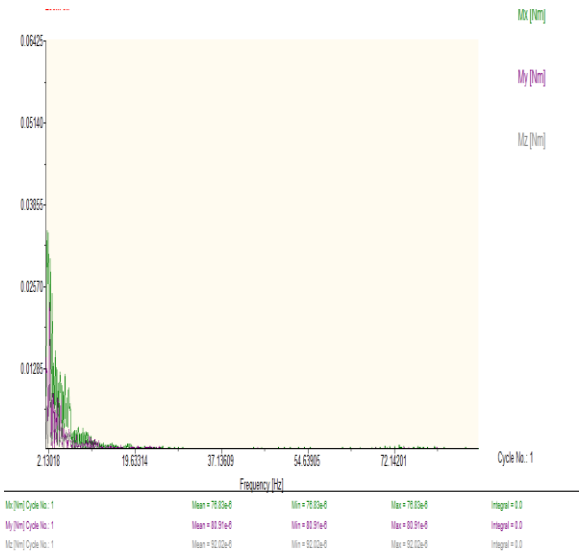

Fig. 13: Plot of the moment of forces and the frequency of the sensor without the use of coolants.

Table 5 presents the magnitude of the cutting force and their corresponding moments in the three orthogonal axes with the use of coolants. Comparing Tables 4 and 5, it was observed that the values of the cutting forces increases without the use of coolants and reduces with the use of coolants. This is due to the fact that without the use of coolants, heat build up at the work piece tool interface increases resulting in increase in temperature within the cutting tool and the work piece. An increase in the temperature of the cutting tool increases the cutting force. Also, the hardness of both the work piece and the cutting tool decreases with increase in the temperature thus increasing the cutting force as well as the shearing rate of the work piece. With increase in temperature, the chips tends to build up around the shearing zone of the work piece making it difficult for the cutting tool to penetrate. This results in poor surface finish. However with the use of coolants, the chips removed are easily flushed out before they build up edges and the heat energy transferred into the cutting tool are easily dissipated without reducing the hardness and the cutting force of the tool. An increase in the temperature of the cutting tool with increase in the cutting force will dull the cutting edges of the tool, reduce the useful life of the tool and promote poor surface finish with resulting increase the machining cycle time.

Tab. 5: Cutting force and moments without the use of coolants.

Run	Time (S)	F_x (N)	F_y (N)	F_z (N)	M_x (Nm)	M_y (Nm)	M_z (Nm)
1	0.000	0.37	1.04	3.17	0.22	0.24	-0.06
2	0.001	0.24	1.65	0.98	0.29	0.24	-0.11
3	0.002	0.49	0.92	4.39	0.22	0.02	-0.07
4	0.003	-0.06	1.16	4.15	0.20	0.22	-0.05
5	0.004	-0.24	1.16	2.20	0.29	0.12	-0.01
6	0.005	-0.06	0.92	2.44	0.24	0.05	-0.01
7	0.006	-0.06	1.16	3.17	0.29	-0.05	-0.12
8	0.007	0.06	1.16	2.93	0.15	0.15	-0.01
9	0.008	0.37	0.79	2.69	0.24	0.07	-0.02
10	0.009	0.31	0.85	3.66	0.20	0.15	-0.01
11	0.010	0.12	0.98	3.42	0.17	0.20	-0.05
12	0.011	0.31	1.10	3.42	0.24	0.12	-0.07
13	0.012	-0.12	0.92	2.69	0.27	0.12	-0.01
14	0.013	0.12	0.85	3.66	0.00	0.34	-0.05
15	0.014	0.31	0.67	3.42	-0.10	0.22	-0.05
16	0.015	-0.12	1.10	2.69	0.10	0.22	-0.01
17	0.016	0.18	1.28	1.71	0.20	0.24	-0.06
18	0.017	0.24	0.22	3.42	0.02	0.24	-0.11
19	0.018	0.24	0.79	3.66	0.24	0.10	-0.04
20	0.019	0.49	1.16	3.91	0.39	0.12	-0.05

Figure 14 shows the orthogonal cutting forces without the use of coolants. The value of the cutting force is highest along the z-axis, followed by the vertical y-axis and least along the horizontal x-axis. When compared with Figure 10, there is significant reduction in the value of the cutting force because of lack of coolants.

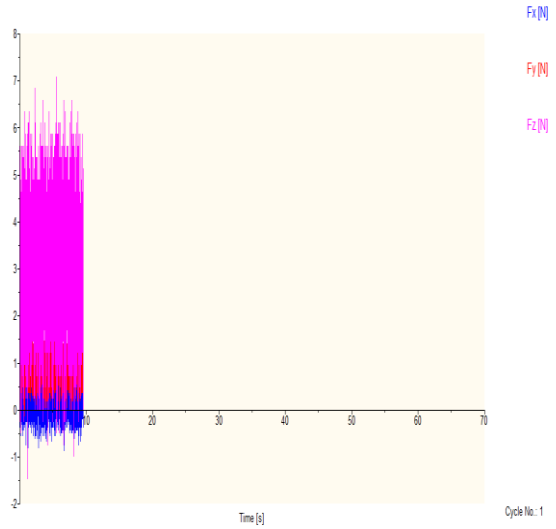

Fig. 14: The three orthogonal cutting force components without the use of coolants.

Figure 15 shows the plot of the three orthogonal cutting forces and the frequency of the sensor without the use of coolants. At high frequencies, the measuring system was able to detect small variations in the values of the cutting forces ranging from 0.00048-0.00241 N.

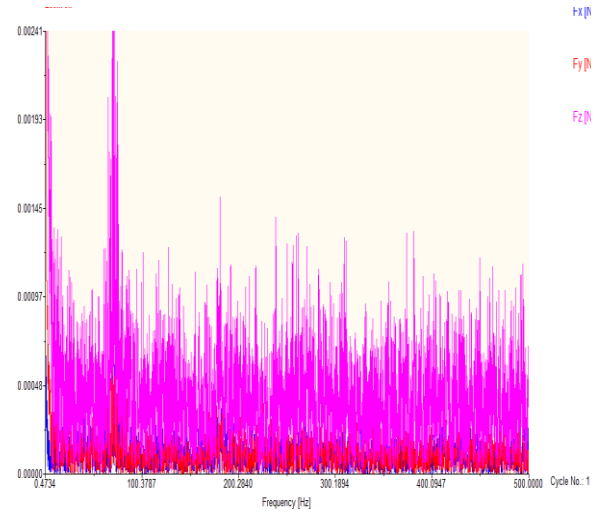

Fig. 15: Plot of the three orthogonal cutting forces and the frequency of the sensor without the use of coolants.

Figure 16 shows the moment of forces in the three orthogonal axes without the use of coolants. Comparing Figures 13 and 17, there was significant increase in the values of the cutting forces due to lack of coolants. The corresponding moment of forces in the three orthogonal axes was also observe to increase. However, the moment of forces was highest along the horizontal x-axis followed by the vertical y-axis and least along the z-axis.

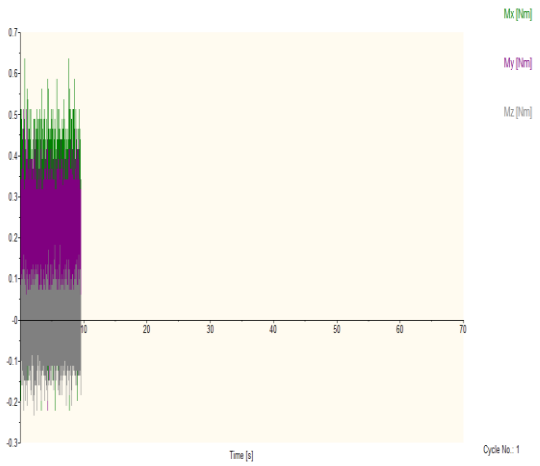

Fig. 16: The moment of forces in the three orthogonal axes without the use of coolants.

Figure 17 shows the plot of the moment of forces and the frequency of the sensor without the use of coolants. At a high frequency, the measuring system was able to compute the small values of the moment of forces thus, indicating that the data acquisition system is highly precise, accurate and sensitive to small measurements and deviations.

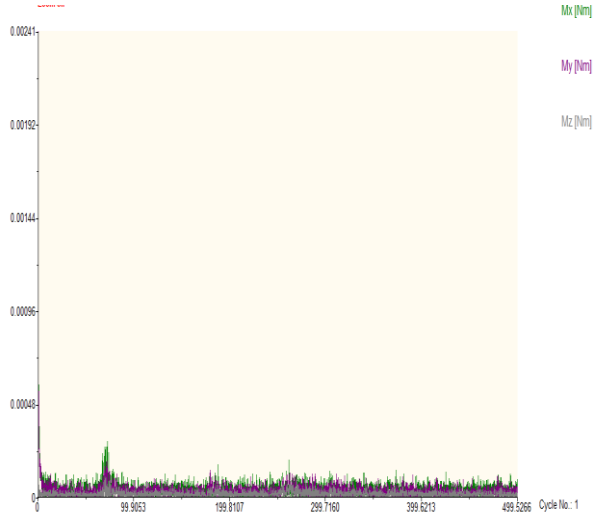

Fig. 17: The plot of the moment of forces and the frequency of the sensor without the use of coolants.

4 CONCLUSION

The modelling and optimization of the cutting forces during the milling process of Ti6Al4V using the response surface methodology and dynamometer was carried out. The statistical analysis of both the numerical and physical experimentation produced a mathematical model for the correlation and prediction of the cutting force as a function of the independent process parameters namely the speed of cut, depth of cut and feed per tooth. The cutting force was found to increase with increase in the depth of cut, feed per tooth, and decrease with

increase in the cutting speed. In addition, the magnitude of the cutting force also increases without the use of coolants and vice versa. The piezo electric force sensors demonstrated high level of precision and accuracy in detecting small variations in the value of the cutting force. The understanding of the variations in the magnitude of the cutting force is essential in the optimization of the overall machining process. Besides, it is an important factor that should be tracked at regular interval as it affects the product surface and dimensional requirements, tool useful life and machinability of the work piece.

5 REFERENCES

[Altintas and Lee, 1996] Altintas, Y and Lee P. A general mechanics and dynamics model for helical end mills. *CIRP Ann. Manuf. Technol.* 1996, 45(1):59–64.

[Altintas, 2012] Altintas, Y. Manufacturing automation: metal cutting mechanics, machine tool vibrations, and CNC design. New York: Cambridge university press, UK, 2012.

[Aouici, 2012] Aouici, H., Yallese, M. A., Chaoui, K., Mabrouki, T., and Rigal, J. F. Analysis of surface roughness and cutting force components in hard turning with CBN Tool. *Measurement.* 2012, 45: 344-353.

[Baohai et al., 2013] Baohai, W., Xue, Ming, L. and Ge, G. Cutting force prediction for circular end milling process. *Chinese Journal of Aeronautics*, 2013, 26(4): 1057–1063.

[Bello et al., 2016] Bello EI, Ogedengbe TI, Lajide L, Daniyan IA. Optimization of process parameters for biodiesel production using response sur-face methodology. *Am. J. Energy Eng*. 2016, 4(2):8–16.

[Burek et al., 2017] Burek, J., Zylka, L., Plodzien, M., Sulkowicz, P. and Buk, J. The effect of the cutting edge helix angle of the cutter on the cutting force components and vibration acceleration amplitude. *Mechanik NR,* 20117, 11:1-3.

[Dikshit et al., 2017] Dikshit, M. A., Puri, A. B., Maity, A. and Banerjee, A. J. Analysis of cutting force and optimization of cutting parameters in high-speed ball end milling using the Response Surface Methodology and the Generic Algorithm. Procedia Materials Science, 2014, 5:1623-1632.

[Ezugwu, and Wang, 1997] Ezugwu, E. O. and Wang, Z. M. Titanium alloys and their machinability – a review, *Journal of Materials Processing Technology*, 1997, 68:262-274.

[Ghorbani and Moetakef-Imani, 2016] Ghorbani, H. and Moetakef-Imani, B. Specific cutting force and cutting condition interaction modeling for round insert face-milling operation. *The International Journal of Advanced Manufacturing Technology*, 2016, 84:1705–1715.

[Giorgio et al., 2016] Giorgio, C. M., Bort, M. Leonesio, P. and Bosetti, A. model-based adaptive controller for chatter mitigation and productivity enhancement in CNC milling machines, *Robot. Comput. Integr. Manuf.* 2016, 40:34–43. http://dx.doi.org/10.1016/j.rcim.2016. 01.006.

[González et al. 2018] González, H., Calleja, A., Pereira, O., Ortega, N., Norberto López de Lacalle, L. and Barton, M. Super abrasive machining of integral rotary components using grinding flank tools. *Metals,* 2018, 8(24):1-11.

[Grossi et al., 2015] Grossi, N., Sallese, L., Scippa, A. and Camptatelli, G. Speed-varying cutting force coefficient identification in milling. *Precision Engineering,* 2015:321-334.

[Jing et al., 2014] Jing, X. B., Li, H. Z., Wang, J. and Tian, Y. L.. Modelling the cutting forces in micro-end-milling using a hybrid approach. *The Intl Journal of Adv Manuf Tech.,* 2014, 73 (9–12): 1647–1656.

[Karabulut, 2015]. Karabulut, Ş.Optimization of surface roughness and cutting force during AA7039/Al 2 O 3 metal matrix composites milling using neural networks and Taguchi method. *Measurement*, 2015, 66:139–149.

[Leal-Muñoza, 2018] Leal-Muñoza, E., Diezb, E., Perezc, H. and Vizana, A. Accuracy of a new online method for measuring machining parameters in milling. *Measurement*, 2018, 128:170–179.

[López de Lacalle et al., 2006] López de Lacalle, L.N., Lamikiz, A., Sánchez, J.A. and Fernández de Bustos I. Simultaneous measurement of forces and machine tool position for diagnostic of machining tests. Department of Mechanical Engineering – University of the Basque Country, Faculty of Engineering of Bilbao, Spain. 2006, pp. 1-21.

[Mehdi and Zghal, 2012] Mehdi, K. and Zghal, A. Modelling cutting force including thrust and tangential damping in peripheral milling process. *Int J Mach Mach Mater*, 2012, 12(3):236–251.

[Mehdi and Zghal, 2011] Mehdi, K. and Zghal, A. "Numerical model for prediction of cutting force in peripheral milling process including thrust and tangential damping", *Advanced Materials Research,* 2011, 223:122-132.

[Mejri and Mehdi, 2018] Mejri, H and and Mehdi, K. Modelling of cutting forces in curvilinear peripheral milling process. *The International Journal of Advanced Manufacturing Technology* doi.org/10.1007/s00170-018-03249-x., 2018

[Nand, 2012] Nandi, A. K. Modelling and analysis of cutting force and surface roughness in milling operation using TSK-Type fuzzy rules. J. of the Braz. Soc. of Mech. Sci. & Eng. January-March 2012, Vol. XXXIV, No. 1:49-61.

[Nurul, 2007)] Nurul, A. K. M. Effectiveness of incoated WC-CO and PCD inserts in end milling of Ti alloy, *Journal of Materials Processing Technology*, 2007, 192-193:147-158.

[Orra and Choudhury, 2015] Orra, K. and Choudhury, S. K. Development of flank wear model of cutting tool by using adaptive feedback linear control system on machining AISI D2 steel and AISI 4340 steel, *Mech. Syst. Signal Process*. 2015, 81:475–492, 2015. http://dx.doi.org/10.1016/j. ymssp.2016.03.011.

[Perez et al., 2013] Perez, H., Diez, E., Marquez, J. J. and Vizan, A. An enhanced method for cutting force estimation in peripheral milling, *Int. J. Adv. Manuf. Technol*. 2013, 69:1731–1741.

[Ratnam et al., 2016] Ratnam, C., Vikram, A. K., Ben, B. S. and Murthy, B. S. N. Process monitoring and effects of process parameters on responses in turn-milling operations based on SN ratio and ANOVA. *Measurement,* 2016, 94:221–232. http://dx.doi.org/10.1016/j. measurement.2016.07.090.

[Ribeiro et al., 2017] Ribeiro, Lopes, H., Queijo, L. and Figueiredo, D. Optimization of cutting parameters to minimize the surface roughness in the end milling process using the Taguchi method, Period. Polytech. Mech. Eng. 2017, 61:30–35. http://dx.doi.org/10.3311/PPme. 9114.

[Rubeo and Schmitz, 2016] Rubeo, M. A. and Schmitz, T. L. Milling force modelling: a comparison of two approaches. *Procedia Manufacturing,* 2016, 5:90-105. doi: 10.1016/j.promfg.2016.08.010.

[Rychkov and Yanyushkin, 2016] Rychkov, D. A. and Yanyushkin, A. S. The methodology of calculation of cutting forces when machining composite materials. VII International Scientific Practical Conference "Innovative Technologies in Engineering" OP Conf. Series: *Materials Science and Engineering.* 2016, 142: 012088, pp. 1-7 doi:10.1088/1757-899X/142/1/012088.

[Scippa et al., 2015] Scippa, A., Sallese, L., Grossi, N. and Campatelli, G. Improved dynamic compensation for accurate cutting force measurements in milling applications. *Mechanical System Signal Process,* 2015, 54-55:314-324.

[Urbikan et al. 2017] Urbikain, G., Artetxe, E. and López de Lacalle, L. N. umerical simulation of milling forces with barrel-shaped tools considering runout and tool inclination angles. *Applied Mathematical Modelling,* 47 (2017) 619–636.

[Wan et al., 2016] Wan, M., Yin, W. and Zhang, W-H. Study on the correction of cutting force measurement with table dynamometer. 9th International Conference on Digital Enterprise Technology-DET2016 “Intelligent Manufacturing in the Knowledge Economy Era” *Procedia CIRP,* 2016, 56:119-123.

[Wen, et al., 2013] Wen, J., Peng, F. Y., Lin, S., Yan, R. and Liu, Y. Z. Cutting force modeling and prediction in end milling including flank wear, *Advanced Materials Research,* 2013, 690-693:2427-2436.

[Wojciechowski et al., 2016] Wojciechowski, S., Maruda, R., Nieslony, P. and Krolczyk, G. M. Investigation on the edge forces in ball end milling of inclined suface. *Int’l Journal of Mech. Sci.* 2016, 119:360-369.

[Yang et al., 2011] Yang, Y., Zhang, W. H. and Wan, M. Effect of cutter runout on process geometry and forces in peripheral milling of curved surfaces with variable curvature. *Int. J. Mach Tools Manuf.* 2011, 51(5):420–427.

[Zhu et al., 2014] Zhu, J. M., Wang, J., Zhang, T. C., Li, X. R. Dynamic milling force measuring method based on cutting tool vibration displacement. *Chinese Journal of Scientific Instrument,* 2014, 35:2772-2782.

[Zhu and Mao et al., 2015] Zhu, M. and Mao, K. M. Multi-channel dynamic force measurement and compensation with inverse filter. *Journal of Xi’an Jiaotong University,* 2015, 49:117-123.